Jurnal Teknologi

Full Paper

NUMERICAL EVALUATION OF CONCRETE FILLED STAINLESS STEEL TUBE FOR SHORT COLUMNS SUBJECTED TO AXIAL COMPRESSION LOAD

Azrul Abd Mutalib*, Mohamed Hamza Mussa, Khaleel Mohammad Khaleel Abusal

Department of Civil and Structural Engineering, University of Kebangsaan Malaysia, 43600 UKM Bangi, Selangor, Malaysia

Article history
Received
20 July 2017
Received in revised form
8 September 2017
Accepted
10 January 2018

*Corresponding author
azrulaam@ukm.edu.my

Graphical abstract

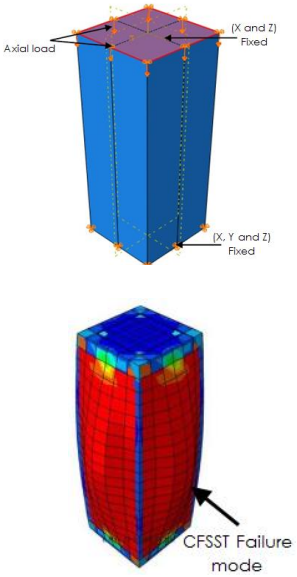

Abstract

Recently, the concrete filled stainless steel tubes (CFSST) columns are widely applied in modern construction due to its aesthetic appearance, high corrosion resistant and less construction cost. The current study aims to evaluate the behavior of CFSST column with square hollow section (SHS) numerically under axial compressive load by using ABAQUS software. A good consistency had achieved between the numerical and experimental test results in terms of load-displacement behaviour and ultimate strength with a maximum difference equal to 2%. Intensive parametric studies had been conducted to determine the effects of stainless steel tubes and concrete properties on the ultimate load capacity of CFSST column. The results proved that the stainless steel tube thickness (t) capable to increase the strength of column by143.59% at t = 10 mm as compared with t = 2 mm, whereas a slight effect had observed for the variation of stainless steel proof stress ($\sigma_{0.2}$). On the other hand, the higher values of concrete strength (fc') obviously reduced the lateral expansion of CFSST column at initial load and led to increase the ultimate load capacity by 34.18 % at fc' = 80 MPa as compared with fc' = 30 MPa. Furthermore, the design strengths calculated according to the Eurocode 4 for concrete filled steel tube (CFST) column appeared a good agreement with the numerical results within an average difference value 2.49%, hence, it could consider as the most rational design method to determine the ultimate strength of CFSST column.

Keywords: CFSST column, stainless steel tube thickness, concrete strength, stainless steel proof stress, numerical analysis

Abstrak

Pada masa ini, tiang tiub keluli terisi konkrit tahan karat (CFSST) digunakan dengan meluas di dalam industri pembinaan moden kerana penampilan estetik, rintangan tahan karat dan kos pembinaan yang rendah. Kajian ini bertujuan untuk menilai kelakuan tiang CFSST empat segi sama berongga (SHS) di bawah beban mampatan dengan menggunakan perisian ABAQUS. Konsistensi yang baik antara keputusan eksperimen dan analisis unsur terhingga telah dicapai dalam aspek kelakuan beban-anjakan dan kekuatan muktamad dengan perbezaan maksimum 2%. Kajian parametrik yang intensif telah dilakukan untuk mendapatkan kesan tiang tiub keluli tahan karat dan sifat konkrit terhadap kapasiti beban muktamad. Keputusan yang didapati membuktikan bahawa ketebalan keluli tiub tahan karat berupaya untuk meningkatkan kekuatan tiang sehingga 14.59% pada t=10mm jika dibandingkan dengan t=2 mm, sedangkan sedikit kesan dapat dilihat untuk variasi tegasan keluli tahan karat ($\sigma_{0.2}$). Sebaliknya, nilai kekuatan konkrit yang tinggi(fc') dengan jelas mengurangkan pemanjangan melintang tiang CFST pada beban permulaan dan menyebabkan kenaikan kapasiti beban muktamad sebanyak 34.18% untuk fc' = 80 MPa jika dibandingkan dengan with fc' = 30 MPa. Tambahan lagi, kekuatan reka bentuk tiang

CFST berpandukan kepada Eurocode 4 menunjukkan persamaan yang sama dengan analis unsur terhingga dengan perbezaan purata sebanyak 2.4%, oleh itu boleh diandaikan bahawa kaedah reka bentuk ini adalah yang paling rasional untuk mendapatkan kekuatan muktamad tiang CCSST.

Keywords: Tiang CFSST, ketebalan besi tahan karat, kekuatan konkrit, tegasan besi tahan karat dan analisis unsur terhinga tahan karat

1.0 INTRODUCTION

Concrete filled steel and stainless steel tubes (CFST and CFSST) are commonly used in modern columns construction practice throughout the world due to the advantages of combining the high compressive strength of concrete with high ductility and tensile resistant of steel as well as their aesthetic appearance, high fire resistant and less construction time [1].

Many experimental and analytical trails had been conducted to investigate the behavior of (CFST) columns with square cross-section under axial compression and flexural loads [2-12], the results appeared a superior strength, stiffness and deformation ability for the square sections of CFST as compared with circular or rectangular sections.

In last decades, the application of stainless steel columns was greatly limited due to the high initial cost in spite of its numerous desirable features such as high corrosion resistant. However, the whole-life cost for a structure has become an important concern by developers which led to encourage using of stainless steel columns. In addition, the composite construction technology had explored an innovative method for utilizing the stainless steel columns in economics manner by filling it with concrete. In this field, extensive experimental studies had been carried out to investigate the behavior of CFSST under different load conditions.

Young and Ellobody [13] evaluated the strength of CFSST with square and rectangular sections under compression axial load. The results were quite conservative for both compact and slender sections with the design strengths predicted based on the American [14] and Australian/New Zealand specifications [15] for cold-formed stainless steel by adopting the material properties of stainless steel obtained from the stub column tests. In addition, two types of failure mode had been observed for CFSST with square sections which were the local buckling failure for the slender sections and a concrete crushing failure mode together with local buckling for specimens with compact sections.

Lam and Gardner [16] determined the compressive behaviour of CFSST columns with square and circular sections filled with concrete infill strengths 30, 60, and 100 MPa. It was found that the existing design rules for carbon steel Eurocode 4 [17] and ACI [18] may generally be safely applied to determine the compressive strength of concrete filled stainless steel tubes, though it tends to be over-conservative. Uy *et al*. [19] determined that the short CFSST columns had a very ductile behavior and higher residual strength under axial compression or the combined actions of axial force as compared with conventional carbon steel CFST columns. However, the CFSST slender columns had showed a similar behaviour in terms of test observations and failure modes with CFST columns. In addition, American code AISC [20] and Eurocode 4 [17] underestimate the load-carrying capacities of CFSST columns under both axial compression and combined actions.

Recently, the numerical solution had provided an efficient alternative to full-scale CFSST columns in order to reduce the cost and time computation. Ellobody and Young [21] developed an finite element model using ABAQUS program to investigate the behaviour and design of axially loaded concrete-filled cold-formed high strength stainless steel tube columns.

Hassanein [22] used ABAQUS program to create a finite element model for lean duplex slender CFSST columns exposed to uniform axial compression program. The results demonstrated that increasing the strength of the concrete core, for the same stainless steel tube, leads, generally, to a linear increase in the strength of the concrete-filled column, at least for the range of concrete strengths investigated herein (25-100) MPa. Tao *et al*. [23] developed a three-dimensional nonlinear finite element using ABAQUS for CFSST columns with square sections under axial compression. The results showed that increased of ultimate strength and ductility of a square CFSST stub column compared with its carbon steel counterpart is mainly due to the contribution of the stainless steel tube, which shows a remarkable strain-hardening characteristics.

Along with previous researches, this paper mainly focused on the numerical evaluation of CFSST columns with square section under axial load using ABAQUS software. The effects of stainless steel tube thickness, concrete compressive strength, and yield stress of stainless steel had been evaluated as well as a further comparison with Eurocode 4 [17] and American code ACI [18] had been carried out.

2.0 METHODOLOGY

2.1 Geometry and Meshing

ABAQUS software was used to create the numerical model of the CFSST column with SHS by adopting the geometrical details of the experimental investigation conducted by Lam and Gardner [16] as described in Table 1 and shown in Figure 1. Where D is the column depth, B is the column width, L is column length, t is column thickness. A_s is cross sectional area of steel tube, A_{eff} is the effective area calculated according to Eurocode 3: Part 1.5 [24], and A_c is the area of concrete. The column length was chosen to be short enough to ensure the overall failure via flexural buckling. In addition, a thin layer of plaster was applied to the two ends of the column in order to achieve uniform axial compressive loading on the top end of column in y direction.

Table 1 Geometry details of CFSST column

Sample	D mm	B mm	L mm	t mm	A_s mm²	A_{eff} mm²	A_c mm²
CFSST	101.3	99.3	300	2	776	494	9269

(a) Test set-up for CFSST column

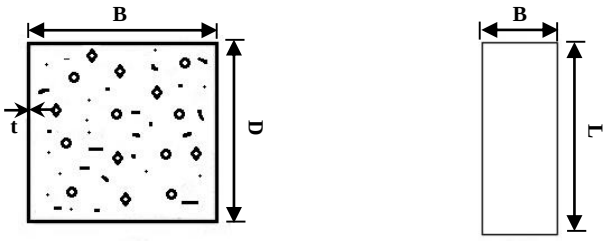

(b) Cross section of CFSST column

Figure 1 Details of experimental test

The four nodes shell element with reduced integration (S4R) had been used to model the stainless steel tube due to its ability to provide six degrees of freedom per each node which could provide accurate solution to numerical model of CFSST columns. On the other hand, the eight nodes brick element (C3D8R) was utilized to model the concrete core, which provides only three translation degrees of freedom and efficiently reduces the running time as well as avoids the shear locking problem.

In numerical model, the thick end plates were in fully connection to the ends of the columns and modeled using three-dimensional four-node bilinear rigid quadrilateral element (R3D4) to decrease CPU-demand on ABAQUS modeling and prevent stress concentration directly below the point of application of the load on top end of the columns. A convergence study was performed to identify an appropriate element size to achieve reliable results with reasonable computation times. In this study, four element sizes were examined 10, 15, 20, and 25 mm with irregular meshing and the results demonstrated that the element size 25 mm able to provide an accurate numerical solution for the CFSST column within a shorten time.

2.2 Material Properties and Modeling

2.2.1 Stainless Steel

The material properties of austenitic stainless steel grade (EN 1.4318) were obtained through the tensile coupon test carried out by Lam and Gardner [16] as presented in Table 2. Where E_0 is the initial Young's modulus, $\sigma_{0.2}$ and $\sigma_{1.0}$ are the 0.2% and 1.0% proof stresses respectively, σ_u is the ultimate tensile strength, and n and $n'_{0.2,1.0}$ are strain hardening exponents for the compound Ramberg–Osgood material model described in [25].

Table 2 Stainless steel material properties

E_0 GPa	$\sigma_{0.2}$ MPa	$\sigma_{1.0}$ MPa	σ_u MPa	n	$n'_{0.2,1.0}$
202.5	385	456	481	12.4	4

Stainless steel alloys characterized by nonexistent yield stress as compared with carbon steel. The Ramberg and Osgood [26] relationship was successfully applied to determine the stress-strain behaviour of stainless steel by adopting the 0.2% proof stress ($\sigma_{0.2}$) as an equivalent yield stress in Eq.1:

$$\varepsilon = \frac{\sigma}{E_0} + 0.002\left[\frac{\sigma}{\sigma_{0.2}}\right]^n \quad \sigma \le \sigma_{0.2} \tag{1}$$

where σ is the value of the measured proof stress, E_0 is the intial Young modulus, $\sigma_{0.2}$ is the 0.2% proof stress, n is sharpness of the stress-strain curve and

could be determined by $\sigma_{0.2}$ and the 0.01 % proof stress $\sigma_{0.01}$ as following:

$$n = \frac{ln\,20}{ln(\sigma_{0.2}/\sigma_{0.01})} \quad (2)$$

It was founded from the previous studies that the Eq.1 could successfully use to determine the stress-strain behaviour of stainless steel up to 0.2% proof stress. Therefore, Rasmussen [25] had proposed a full range stress-strain relationship which significantly assisted to predict the stress-strain behaviour of stainless steel beyond 0.2% proof stress:

$$\varepsilon = \frac{\sigma - \sigma_{0.2}}{E_{0.2}} + \varepsilon_u \left(\frac{\sigma - \sigma_{0.2}}{\sigma_u - \sigma_{0.2}}\right)^m + \varepsilon_{0.2} \quad For\ \sigma > \sigma_{0.2} \quad (3)$$

$$E_{0.2} = \frac{E}{1 + 0.002\,n/e} \quad (4)$$

$$e = \frac{E_0}{\sigma_{0.2}} \quad (5)$$

$$m = 1 + 3.5\frac{\sigma_{0.2}}{\sigma_u} \quad (6)$$

$$\frac{\sigma_{0.2}}{\sigma_u} = \frac{0.2 + 185e}{1 - 0.0375(n-5)} \quad (7)$$

$$\varepsilon_u = 1 - \frac{\sigma_{0.2}}{\sigma_u} \quad (8)$$

$$\varepsilon_{0.2} = \frac{\sigma_{0.2}}{E_0} + 0.002 \quad (9)$$

In this study, the Ramberg – Osgood expression Eq. 1 was used to determine the stress-strain behavior of stainless steel for the stresses up to 0.2% proof stress, and Rasmussen expression Eq.3 was applied for the stresses beyond the 0.2 % proof stress. ABAQUS software is usually defined the material stress–strain relationship in terms of true stress σ and logarithmic plastic true strain ε^{pl}_{true}. Therefore, the nominal values of stress (σ) and strain (ε) had been converted to a true stress–strain relationship by using the following equations:

$$\sigma_{true} = \sigma(1 + \varepsilon) \quad (10)$$

$$\varepsilon^{pl}_{true} = ln(1 + \varepsilon) - \frac{\sigma_{true}}{E_0} \quad (11)$$

2.2.2 Concrete

During the experimental test, the mean measured cube strength for C60 was 66 MPa, whilst the corresponding cylinder strength was 53 MPa [16]. The damage plasticity model [27] was used to simulate the confined core concrete by using an equivalent stress-strain relationship proposed by Han *et al*. [28] for core concrete in CFST under compression load and replacing the yield strength (f_y) of carbon steel by the 0.2% proof stress $\sigma_{0.2}$ in Eq. 12:

$$\frac{\sigma}{f_c'} = \begin{cases} 2\frac{\varepsilon}{\varepsilon_0} - \left(\frac{\varepsilon}{\varepsilon_0}\right)^2 & \frac{\varepsilon}{\varepsilon_0} \le 1 \\ \dfrac{\frac{\varepsilon}{\varepsilon_0}}{B_0\left(\frac{\varepsilon}{\varepsilon_0} - 1\right)^{\eta} + \frac{\varepsilon}{\varepsilon_0}} & \frac{\varepsilon}{\varepsilon_0} > 1 \end{cases} \quad (12)$$

where f_c' is the cylinder compressive strength of concrete, ε_0, B_0, and η are model parameters depend on the confinement factor ξ which used to represent the increament in the plastic behaviour due to the passive confinement of steel tube and could be determine as following:

$$\xi = \frac{A_s f_y}{A_c f_{ck}} = \alpha\,\frac{\sigma_{0.2}}{f_{ck}} \quad (13)$$

In which $\alpha = \frac{A_S}{A_c}$ is the steel ratio, $\sigma_{0.2}$ is 0.2% proof stress for stainless steel, and f_{ck} = 0.67f_{cu} , where f_{cu} is the cube strength of concrete.

2.2.3 Loading and Boundary Conditions

A uniform axial compressive force was applied at the top end of the CFSST column by using the modified Riks method (STATIC, RIKS) option available in the ABAQUS library to ensure the smooth increments of loading without undesired bifurcations. The ends of the stub column were fixed against all degrees of freedom except for the vertical displacement at the top end as shown in Figure 2. Moreover, the contact between steel and concrete was modeled by interface elements, using the (CONTACT PAIR) option by surface-to-surface type and finite sliding formulation, available within the ABAQUS element library.

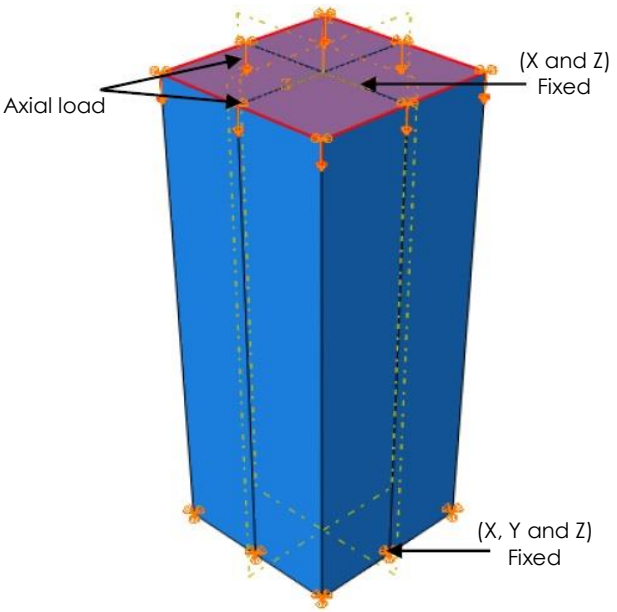

Figure 2 Boundary conditions of CFSST

3.0 RESULTS AND DISCUSSION

3.1 Verification

To ensure the accuracy of the numerical model, a comparison had been achieved with available experimental results determined by Lam and Gardner [16] for CFSST column with SHS. The results proved a good consistency in term of the load-displacement behavior for the CFSST column within maximum difference in the ultimate load capacity reach up to 2% as presented in Figure 3.

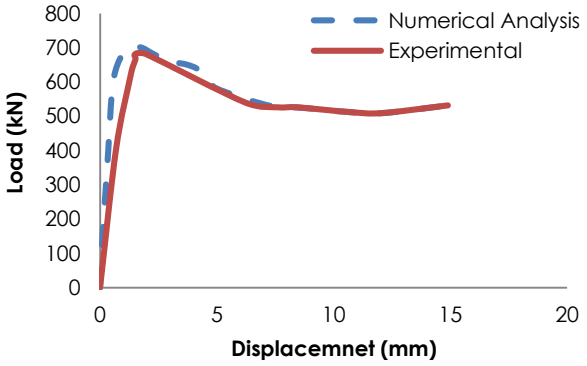

Figure 3 Comparison between numerical and experimental results

Moreover, Figure 4 had showed an acceptable agreement between the numerical deformed and the typical failure mode of CFSST column observed during the experimental investigation. From the above comparisons, it can be found that the numerical solution could successfully applied to achieve further analysis and parametrical studies on the CFSST column within short time an d less cost computation.

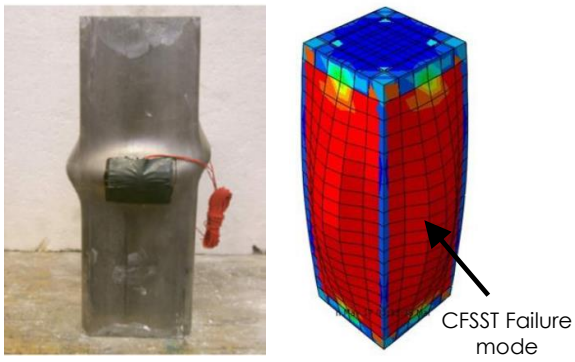

Figure 4 Comparison of experimental and numerical failure modes

3.2 Parametric Studies

Intensive parametric studies had been created out on the numerical model CFSST which has the following basic parameters: L = 300 mm, B = 101.3 mm, t = 2 mm, austenitic stainless steel grade (EN 1.4318), $\sigma_{0.2}$ = 385 MPa, E_0 = 202.5 GPa, n = 12.4, and fc' = 53 MPa.

3.2.1 Effect of Stainless Steel Tube Thickness (t)

Currently, various stainless steel tube thicknesses are usually used in the design of CFSST column and the inaccurate thickness choice could significantly effect on the ultimate load capacity of CFSST and construction cost. Therefore, intensive parametric study had been conducted on the CFSST numerical model by testing four thicknesses of stainless steel tube (4, 6, 8, and 10) mm filled up by concrete C60.

Table 3 demonstrated that the increment of stainless steel tube thickness could significantly increase the ultimate load resistant (P_u) of CFSST column and the maximum value of increment percentage achieved at t = 10 mm by 143.59% as compared with t = 2 mm. However, utilizing of thicker stainless steel tube could highly increase the initial cost of the CFSST column which means that the thinner stainless steel such as t = 6 mm could be the desire choice for designer to ensure highly load resistant capacity within less construction cost.

Table 3 Effect of stainless steel tube thickness (t) on ultimate load (P_u) of CFSST column

Sample	t (mm)	P_u (kN)	Percentage %
CFSST	2	702	-
CFSST 1	4	1025	46.01
CFSST 2	6	1269	80.77
CFSST 3	8	1482	111.1

In addition, it was found that the stainless steel tube thickness could have a positive effect on the ductility index (DI) of the CFSST column as shown in Figure 5, which could obviously enhance the resistant of tube against high values of compression axial load and reduce the end shortening of the column.

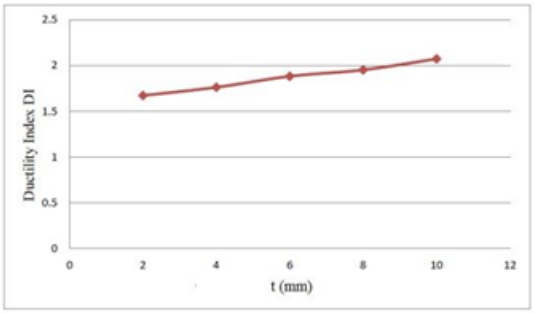

Figure 5 Effect of stainless steel tube thickness (t) on the ductility index (DI)

3.2.2 Effect of Stainless Steel Proof Stress ($\sigma_{0.2}$)

Various grade of stainless steel are usually used by engineers to design CFSST column and the choice of the desire grade depending on the heat treatment, chemical composition, and yield strength. Generally, the stainless steel can be classified into three types according to Eurocode 3 [29] which are ferritic, austenitic and duplex stainless steel. Therefore, further evaluation had been carried out on the numerical model CFSST by using another types of stainless steel tube which were ferritic stainless steel grade (EN 1.4003) has $\sigma_{0.2}$ = 280 MPa, and duplex stainless steel grade (EN 1.4362) with $\sigma_{0.2}$ = 420 MPa. In addition, the variation effects of initial Young's modulus (E_0) and strain hardening parameter (n) had been neglected according to insignificant influence of these parameters on the load capacity of CFSST column Tao *et al*. [23]. Table 4 appeared slight influence of the stainless steel proof stress ($\sigma_{0.2}$) on the ultimate load capacity of CFSST column. The ferritic stainless steel type had reduced the ultimate load by 10.03% as compared with austenitic type, whereas, the duplex stainless steel type had appeared slight increasing by 1.85% without any obvious difference in the behavior of the load-axial shortening of columns in all the investigated cases.

Table 4 Effect of stainless steel proof stress ($\sigma_{0.2}$) on ultimate load capacity (P_u) of CFSST column

Sample	Type	$\sigma_{0.2}$	Pu (kN)	Percentage %
CFSST	Austenitic	385	702	-
CFSST 9	Ferritic	280	638	10.03
CFSST 10	Duplex	420	715	1.85

3.2.3 Effect of Concrete Strength (fc')

Further investigation had been conducted on the CFSST numerical model to evaluate the effects of concrete strength (fc') on the ultimate strength of CFSST column by utilizing four values of (fc') 30, 50, 70, and 80 MPa. It was found that the higher values of concrete strength could significantly reduce the lateral expansion of CFSST column at the initial load stage which indicates that the interaction between the concrete and stainless steel tube could postpone when the (fc') increases. Moreover, Table 5 proved that lower values of (fc') could clearly decrease the ultimate load capacity of CFSST column by 58.82 % at fc' = 30 MPa as compared with fc' = 53 MPa, whereas the higher values of concrete strength could obviously raise the load resistant by 34.18 % in case of fc' = 80 MPa which lead to increase the ductility index (ID) of the CFSST column under compression load effect.

Table 5 Effect of concrete strength fc' ultimate load capacity (P_u) of CFSST column

Sample	fc' (MPa)	Pu (kN)	Percentage %
CFSST	53	702	-
CFSST 5	30	442	58.82
CFSST 6	40	527	24.93
CFSST 7	70	847	20.66

3.3 Comparison of Parametric Study Results with Existing Design Codes

Up to date, there is no specific design code could be used to determine the ultimate load capacity of CFSST column. Therefore, the design equations available in Eurocode 4 [30] and American code ACI [18] for CFST column are widely used to calculate the load capacity of CFSST with SHS under compressive loads by replacing the yield stress of carbon steel (f_y) with 0.2% proof stress ($\sigma_{0.2}$) and utilizing the effective area of steel mentioned in Table 1 above :

$$P_{EC4} = A_c f_c + A_{eff} f_y \quad \text{Eurocode 4} \tag{14}$$

$$P_{ACI} = 0.85 A_c f_c + A_{eff} f_y \quad \text{ACI code} \tag{15}$$

where A_c is the cross-sectional area of the concrete, f_c is the compressive concrete cylinder strength, A_{eff} is the effective area of the steel and f_y is the yield strength of the steel. Table 6 showed a comparison between the design load strengths (P_{EC4} and P_{ACI}) and parametric studies results obtained from the variation of stainless steel tube thickness (t) between 2 - 10 mm, concrete strength (fc') range from 30 to 80 MPa and proof stress ($\sigma_{0.2}$) between 280 - 420 MPa.

Table 6 Comparison between parametric studies and design codes results

Sample	$P_{num.}$ (kN)	P_{EC4} (kN)	P_{ACI} (kN)	Difference %	
				EC4	ACI
CFSST	702	681.64	607.92	2.90	15.47
CFSST 1	1025	1044.67	976.96	1.91	4.91
CFSST 2	1269	1284.51	1222.54	1.22	3.80
CFSST 3	1482	1513.72	1457.24	2.14	1.69
CFSST 4	1710	1732.31	1681.06	1.30	1.7
CFSST 5	442	468.37	426.64	5.96	3.60
CFSST 6	527	561.09	505.46	6.47	4.26
CFSST 7	847	839.27	741.91	0.92	14.16
CFSST 8	942	932.01	820.73	1.07	14.77
CFSST 9	638	629.77	556.05	1.30	14.74
CFSST 10	715	698.93	625.21	2.30	14.36

The outcomes proved that the Eurocode 4 and ACI codes could give conservative predictions for the ultimate load capacity of CFSST columns at different values of (t), (fc'), and ($\sigma_{0.2}$). Nevertheless, Eurocode 4 had appeared the best predictions for the ultimate load within an average value 2.49% which seems as the most rational design method

may be put forward to predict the section capacities of CFSST column with SHS.

4.0 CONCLUSION

The verification study appeared a good consistency with the available experimental results of CFSST column in terms of the load-displacement behaviour and failure mode within a maximum error value in ultimate load capacity reach up to 2%.The validity of the present formulation is verified with existing modeled and experimental results.

The variation of stainless steel tube thickness (t) had caused a significant rising in ultimate load capacity and ductility index (DI) of CFSST column within maximum increment 143.59% at t = 10 mm as compared with t = 2 mm. Nevertheless, it was recommended to utilize the t = 6 mm to reduce the initial high cost of stainless steel.

The lower values of concrete strength (fc') clearly decreased the load capacity of CFSST by 58.82 % at fc' = 30 MPa as compared with fc' = 53 MPa, whereas, the highest values had obviously reduced the lateral expansion of CFSST column at initial load and increased the ultimate load of column by 34.18 % at fc' = 80 MPa.

The stainless steel proof stress ($\sigma_{0.2}$) had showed slightly influence on the load strength capacity of CFSST column specially in case of duplex stainless steel which the ultimate load increased by only 1.85% as compared with austenitic type.

The existing design formulas available in Eurocode 4 for CFST column proved their worth as the most rational design method to predict the ultimate load of CFSST column within an average value 2.49%.

Acknowledgement

The authors would like to acknowledge the financial support from grant number AP-2015-011 and the Fundamental Research Grant Scheme (grant number FRGS/1/2015/TK01/UKM/02/4) to perform this research.

References

[1] Han, L.-H., Li, W. and Bjorhovde, R. 2014. Developments and Advanced Applications of Concrete-filled Steel Tubular (CFST) Structures: Members. *Journal of Constructional Steel Research*. 100: 211-228.

[2] Giakoumelis, G. and Lam, D. 2004. Axial Capacity of Circular Concrete-filled Tube Columns. *Journal of Constructional Steel Research*. 60(7): 1049-1068.

[3] Han, L.-H., Zhao, X.-L., and Tao, Z. 2001. Tests and Mechanics Model for Concrete-filled SHS Stub Columns, Columns and Beam-columns. *Steel and Composite Structures*. 1(1): 51-74.

[4] Han, L.-H. 2002. Tests on Stub Columns of Concrete-filled RHS Sections. *Journal of Constructional Steel Research*. 58(3): 353-372.

[5] Tao, Z., Han, L.-H. and Wang, Z.-B. 2005. Experimental Behaviour of Stiffened Concrete-filled Thin-walled Hollow Steel Structural (HSS) Stub Columns. *Journal of Constructional Steel Research*. 61(7): 962-983.

[6] Lee, S.-H. 2011. Behavior of High-strength Circular Concrete-filled Steel Tubular (CFST) Column Under Eccentric Loading. *Journal of Constructional Steel Research*. 67(1): 1-13.

[7] Perea, T. 2014. Full-scale Tests of Slender Concrete-filled Tubes: Interaction Behavior. *Journal of Structural Engineering*. 140(9): 04014054.

[8] Han, L.-H., Yao, G.-H. and Tao, Z. 2007. Behaviors of Concrete-filled Steel Tubular Members Subjected To Combined Loading. *Thin-walled Structures*. 45(6): 600-619.

[9] Shanmugam, N. E., Lakshmi, B. and Uy, B. 2002. An Analytical Model for Thin-walled Steel Box Columns with Concrete In-fill. *Engineering Structures*. 24(6): 825-838.

[10] Han, L.-H. 2004. Flexural Behaviour of Concrete-filled Steel Tubes. *Journal of Constructional Steel Research*. 60(2): 313-337.

[11] Ellobody, E. and Young, B. 2006. Nonlinear Analysis Of Concrete-filled Steel SHS and RHS Columns. *Thin-walled Structures*. 44(8): 919-930.

[12] Tao, Z. 2009. Analysis and Design of Concrete-filled Stiffened Thin-walled Steel Tubular Columns Under Axial Compression. *Thin-Walled Structures*. 47(12): 1544-1556.

[13] Young, B. and Ellobody, E. 2006. Experimental Investigation of Concrete-filled Cold-formed High Strength Stainless Steel Tube Columns. *Journal of Constructional Steel Research*. 62(5): 484-492.

[14] Rasmussen, K. and Hancock, G. 1993. Design of Cold-formed Stainless Steel Tubular Members. I: Columns. *Journal of Structural Engineering*. 119(8): 2349-2367.

[15] Standard, A. and N. Z. Standard, 2001. Cold-formed Stainless Steel Structures. *AS/NZS*. 4673.

[16] Lam, D. and L. Gardner. 2008. Structural Design of Stainless Steel Concrete Filled Columns. *Journal of Constructional Steel Research*. 64(11): 1275-1282.

[17] de Normalisation, C. E. 1994. Eurocode 4: Design of Composite Steel and Concrete Structures. Part 1-2: General Rules-structural Fire Design. European Committee for Standardization (CEN) ENV.

[18] Committee, A., A. C. Institute, and I. O. f. Standardization. 2008. *Building Code Requirements for Structural Concrete (ACI 318-08) and Commentary*. American Concrete Institute.

[19] Uy, B. Tao, , Z. and Han, L.-H. 2011. Behaviour of Short and Slender Concrete-filled Stainless Steel Tubular Columns. *Journal of Constructional Steel Research*. 67(3): 360-378.

[20] ANSI, B. 2005. *AISC 360-05-Specification for Structural Steel Buildings*. Chicago! AISC.

[21] Ellobody, E. and Young, B. 2006. Design and Behaviour of Concrete-filled Cold-formed Stainless Steel Tube Columns. *Engineering Structures*. 28(5): 716-728.

[22] Hassanein, M. 2010. Numerical Modelling of Concrete-filled Lean Duplex Slender Stainless Steel Tubular Stub Columns. *Journal of Constructional Steel Research*. 66(8): 1057-1068.

[23] Tao, Z. 2011. Nonlinear Analysis of Concrete-filled Square Stainless Steel Stub Columns Under Axial Compression. *Journal of Constructional Steel Research*. 67(11): 1719-1732.

[24] Kuhlmann, U., L. Davaine, and B. Braun. 2012. *Design of Plated Structures: Eurocode 3: Design of Steel Structures, Part 1-5: Design of Plated Structures*. John Wiley & Sons.

[25] Rasmussen, K. J. 2003. Full-range Stress–strain Curves for Stainless Steel Alloys. *Journal of Constructional Steel Research*. 59(1): 47-61.

[26] Ramberg, W. and W. R. Osgood. 1943. *Description of Stress-strain Curves by Three Parameters*.

[27] Version, A.S.U.s.M., 6.9. 2009. *Pawtucket, RI: Hibbit, Karlsson & Sorensen*. Inc.

[28] Han, L.-H., Yao, G.-H. and Tao, Z. 2007. Performance of Concrete-filled Thin-walled Steel Tubes Under Pure Torsion. *Thin-Walled Structures.* 45(1): 24-36.
[29] Eurocode, E. 1993. *3: Design of Steel Structures–Part 1.4: General Rules–supplementary Rules for Stainless Steels.* British Standards Institution, BS EN. 1-4.
[30] EN, C. 2004. *1–1. Eurocode 4: Design of Composite Steel and Concrete Structures—Part 1.1: General Rules and Rules for Buildings.* Brussels: European Committee for Standardization.